A&A 493, 645–650 (2009)
DOI: 10.1051/0004-6361:200810557

Astronomy & Astrophysics

The HARPS search for southern extra-solar planets⋆

XIV. Gl 176b, a super-Earth rather than a Neptune, and at a different period

T. Forveille[1], X. Bonfils[2,1,3], X. Delfosse[1], M. Gillon[4], S. Udry[4], F. Bouchy[5], C. Lovis[4], M. Mayor[4], F. Pepe[4], C. Perrier[1], D. Queloz[4], N. Santos[2], and J.-L. Bertaux[6]

[1] Laboratoire d'Astrophysique de Grenoble, Observatoire de Grenoble, Université Joseph Fourier, CNRS, UMR 571, 38041 Grenoble cedex 09, France
e-mail: Thierry.Forveille@obs.ujf-grenoble.fr
[2] Centro de Astrofísica, Universidade do Porto, Rua das Estrelas, 4150-762 Porto, Portugal
[3] Centro de Astronomia e Astrofísica da Universidade de Lisboa, Observatório Astronómico de Lisboa, Tapada da Ajuda, 1349-018 Lisboa, Portugal
[4] Observatoire de Genève, Université de Genève, 51 ch. des Maillettes, 1290 Sauverny, Switzerland
[5] Institut d'Astrophysique de Paris, CNRS, Université Pierre et Marie Curie, 98bis Bd. Arago, 75014 Paris, France
[6] Service d'Aéronomie du CNRS, BP 3, 91371 Verrières-le-Buisson, France

Received 10 July 2008 / Accepted 3 September 2008

ABSTRACT

A 10.24-day Neptune-mass planet was recently announced as orbiting the nearby M2 dwarf Gl 176, based on 28 radial velocities measured with the HRS spectrograph on the Hobby-Heberly Telescope. We obtained 57 radial velocities of Gl 176 with the ESO 3.6 m telescope and the HARPS spectrograph, which is known for its sub-m s^{-1} stability. The median photon-noise standard error of our measurements is 1.1 m s^{-1}, significantly lower than the 4.7 m s^{-1} of the HET velocities, and the 4-year period over which they were obtained overlaps considerably with the epochs of the HET measurements. The HARPS measurements show no evidence of a signal at the period of the putative HET planet, suggesting that its detection was spurious. We do find, on the other hand, strong evidence of a lower mass 8.4 $M_{\rm Earth}$ planet, in a quasi-circular orbit and at the different period of 8.78 days. The host star has moderate magnetic activity and rotates on a 39-day period, which we confirm through modulation of both contemporaneous photometry and chromospheric indices. We detect that period, as well, in the radial velocities, but it is well removed from the orbital period and offers no cause for confusion. This new detection of a super-Earth ($2\ M_{\rm Earth} < M \sin(i) < 10\ M_{\rm Earth}$) around an M dwarf adds to the growing evidence that such planets are common around very low-mass stars. A third of the 20 known planets with $M \sin(i) < 0.1\ M_{\rm Jup}$ and 3 of the 7 known planets with $M \sin(i) < 10\ M_{\rm Earth}$ orbit an M dwarf, in contrast to just 4 of the ~300 known Jupiter-mass planets.

Key words. stars: planetary systems – stars: late-type – stars: activity – stars: low-mass, brown dwarfs – stars: starspots – stars: individual: G1 176

1. Introduction

Of the ~250 planetary systems currently known from radial velocity monitoring, just half a dozen are centered around M dwarfs ($M < 0.6\,M_\odot$)[1]. This in part reflects a selection bias, since an order of magnitude fewer faint M dwarfs are searched for planets than are brighter solar-type stars, but M dwarfs also seem to genuinely have fewer massive planets ($\sim M_{\rm Jup}$) than the more massive solar-type stars do (Bonfils et al. 2006; Johnson et al. 2007). They seem, on the other hand, (Bonfils et al. 2006) to have a larger number of the harder to detect Neptune-mass and super-Earth planets: a third of the ~20 planets with $M \sin(i) < 0.1\ M_{\rm Jup}$ known to date orbit an M dwarf, in spite of solar-type stars outnumbering those by an order of magnitude in planet-search samples. As a consequence of their small overall number, each individual M-dwarf planetary system still plays a significant role in defining these emerging statistical properties.

Very recently, Endl et al. (2008) announced the discovery of a planet with a minimum mass of $M \sin(i) = 25\ M_{\rm Earth}$ in a 10.24-day orbit around a nearby M2.5 dwarf, Gl 176 (Table 1). Gl 176 (also HD 285968, HIP 21932, LHS 196) is a $V = 9.97$ (Upgren 1974) member of the immediate solar neighborhood (par = 106.2 ± 2.5 mas, $d = 9.4$ pc, Perryman & ESA 1997). The 2MASS photometry (Skrutskie et al. 2006) and the parallax result in an absolute magnitude of $M_{Ks} = 5.74$, which the K-band mass-luminosity relation of Delfosse et al. (2000) translates to a mass of $0.50\,M_\odot$. Based on the Bonfils et al. (2005) photometric metallicity calibration, [Fe/H] is –0.1 ± 0.2 and therefore solar within its uncertainty.

We have independently been monitoring the radial velocity of Gl 176 using the HARPS spectrograph on the ESO 3.6-m telescope, over a period that overlaps the epochs of the Endl et al. (2008) observations. Section 2 describes those independent measurements and concludes that they do not confirm the 10.24-day planet. Section 3 takes a closer look at those mesurements and finds that they contain two coherent signals, with periods of 8.78 and 40.0 days. Section 4 discusses differential photometry and the variation in chromospheric indices, to conclude that the

⋆ Based on observations made with the HARPS instrument on the ESO 3.6-m telescope at La Silla Observatory under program ID 072.C-0488.
[1] http://exoplanet.eu/catalog-RV.php

Table 1. Observed and inferred stellar parameters for Gl 176.

Parameter		Gl 176
Spectral type		M2V
V		9.97 ± 0.03
π	[mas]	106.16 ± 2.51
Distance	[pc]	9.42 ± 0.22
M_V		10.10 ± 0.06
K		5.607 ± 0.034
M_K		5.74 ± 0.06
$L_\star$	[$L_\odot$]	0.022
$L_x/L_{\rm bol}$		3.5×10^{-5}
$v \sin i$	[km s^{-1}]	≲0.8
[Fe/H]		−0.1 ± 0.2
$M_\star$	[$M_\odot$]	0.50

40-day signal reflects the stellar rotation period. The 8.78-day period, on the other hand, is due to a bona fide planet, with a minimum mass of only 8.4 $M_{\rm Earth}$. Section 5 concludes with a brief discussion of the new planet.

2. HARPS Doppler measurements and orbital analysis

We observed Gl 176 with HARPS (High Accuracy Radial velocity Planet Searcher) as part of the guaranteed-time program of the instrument consortium. HARPS is a high-resolution (R = 115 000) fiber-fed echelle spectrograph, optimized for planet search programs and asteroseismology. It is the most precise spectro-velocimeter to date, with a long-term instrumental RV accuracy under 1 m s^{-1} (Mayor et al. 2003; Santos et al. 2004; Lovis et al. 2005). When it aims for ultimate radial velocity precision, HARPS uses simultaneous exposures of a thorium lamp through a calibration fiber. For our M dwarf program however, we rely instead on its very high instrumental stability (nightly instrumental drifts <1 m s^{-1}). Most M dwarfs are too faint for us to reach the stability limit of HARPS within realistic integration times, and dispensing with the simultaneous thorium light produces much cleaner stellar spectra, suitable for quantitative spectroscopic analyses.

For the V = 9.97 Gl 176, we used 15 mn exposures, and the median S/N ratio of our 57 spectra is 60 per pixel at 550 nm. The radial velocities (Table 2) were obtained with the standard HARPS reduction pipeline, based on cross-correlation with a stellar mask and a precise nightly wavelength calibration from ThAr spectra (Lovis & Pepe 2007). They have a median internal error of only 1.1 m s^{-1}, which includes both the nightly zero-point calibration uncertainty (∼0.5 m s^{-1}) and the photon noise, computed from the full Doppler information content of the spectra (Bouchy et al. 2001).

The computed velocities exhibit an rms dispersion of 5.3 m s^{-1}. This is far above the 1 m s^{-1} internal errors and significantly more than we observe for stars with similar chromospheric activity, but less than the ∼8 m s^{-1} expected from the 11.7 m s^{-1} velocity amplitude of the Endl et al. (2008) orbit. Figure 1 confirms that the HARPS velocities are more tightly packed than both the HET measurements (top panel) and the predictions of the Endl et al. (2008) orbit (lower panel). Its lower panel demonstrates that they do not phase on the Endl et al. (2008) period, and we verified that the subset of the HARPS dataset that overlaps the published HET measurements does not either. Since any instrumental or astrophysical noise can only increase the velocity dispersion, and can never decrease it, the HARPS measurements set a ∼7.5 m s^{-1} ceiling on the radial velocity amplitude of a Keplerian orbit (except for unrealistically high eccentricities). This forces us to conclude that the Endl et al. (2008) orbit must be spurious, though we do not have a ready explanation for why.

Table 2. Radial-velocity measurements and error bars for Gl 176. All values are relative to the solar system barycenter, and corrected from the small perspective acceleration using the Hipparcos parallax and proper motion.

JD-2 400 000	RV [km s^{-1}]	Uncertainty [km s^{-1}]
52 986.713028	26.4097	0.0024
53 336.797232	26.4133	0.0018
53 367.703446	26.4080	0.0010
53 371.679444	26.4146	0.0012
53 372.672289	26.4150	0.0011
53 373.698683	26.4149	0.0016
53 375.708263	26.4074	0.0011
53 376.644426	26.4074	0.0011
53 377.637888	26.4072	0.0010
53 378.667446	26.4114	0.0013
53 674.790011	26.4012	0.0010
53 693.724506	26.4120	0.0011
53 695.679077	26.4167	0.0009
53 697.762057	26.4217	0.0016
53 699.629044	26.4154	0.0011
53 721.725478	26.4120	0.0014
53 725.600014	26.4082	0.0014
53 727.617518	26.4069	0.0012
53 784.533236	26.4056	0.0011
53 786.526663	26.4068	0.0010
53 809.529447	26.4176	0.0011
53 810.515057	26.4184	0.0010
53 811.510284	26.4211	0.0011
53 812.506114	26.4200	0.0013
53 813.507893	26.4148	0.0011
53 814.507265	26.4123	0.0011
53 815.501823	26.4106	0.0012
53 817.502490	26.4110	0.0010
54 048.826783	26.4184	0.0010
54 050.768921	26.4114	0.0009
54 052.748970	26.4067	0.0011
54 054.812777	26.4093	0.0010
54 078.698716	26.4005	0.0009
54 080.713033	26.4065	0.0012
54 082.712795	26.4123	0.0012
54 084.737341	26.4136	0.0014
54 114.597344	26.4051	0.0014
54 117.631291	26.4122	0.0010
54 122.584109	26.4097	0.0010
54 135.548955	26.4141	0.0010
54 140.552388	26.4040	0.0010
54 142.585254	26.4095	0.0010
54 166.508802	26.4099	0.0011
54 168.505999	26.4141	0.0010
54 170.501820	26.4194	0.0011
54 174.499424	26.4092	0.0012
54 342.888384	26.4068	0.0011
54 345.866037	26.4087	0.0010
54 385.842984	26.3989	0.0013
54 386.803603	26.4015	0.0015
54 387.840396	26.4044	0.0012
54 390.838236	26.4087	0.0012
54 392.803574	26.4030	0.0011
54 393.820127	26.4044	0.0011
54 394.817280	26.4029	0.0012
54 423.739978	26.4045	0.0013
54 428.729841	26.4096	0.0010

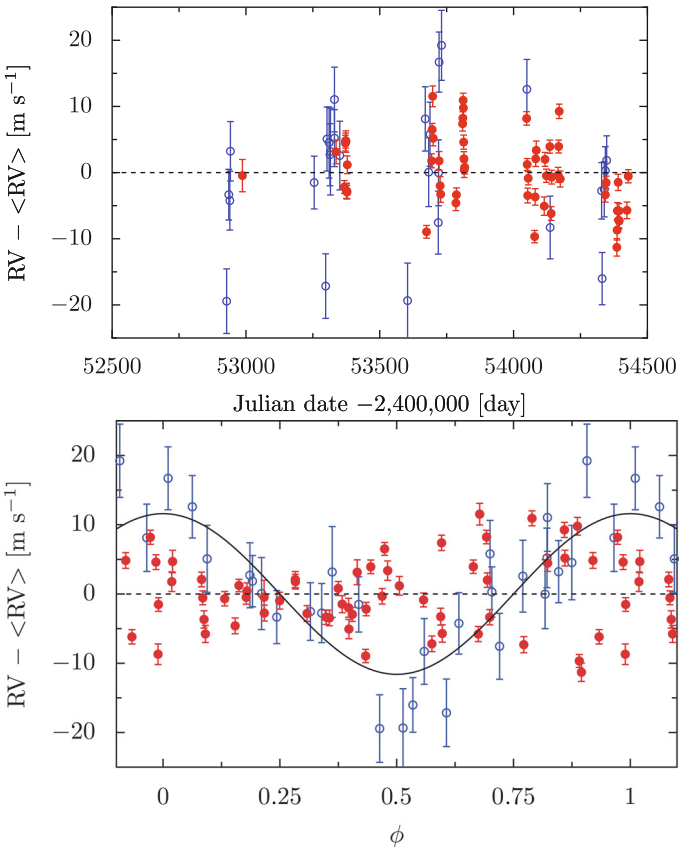

Fig. 1. *Top panel*: HARPS (red filled symbols) and Endl et al. (2008) (blue empty symbols) radial velocities of Gl 176 as a function of time. *Bottom panel*: HARPS radial velocities phased at the 10.24-day period of the Endl et al. (2008) orbit, overlaid with the radial velocity prediction for that orbit.

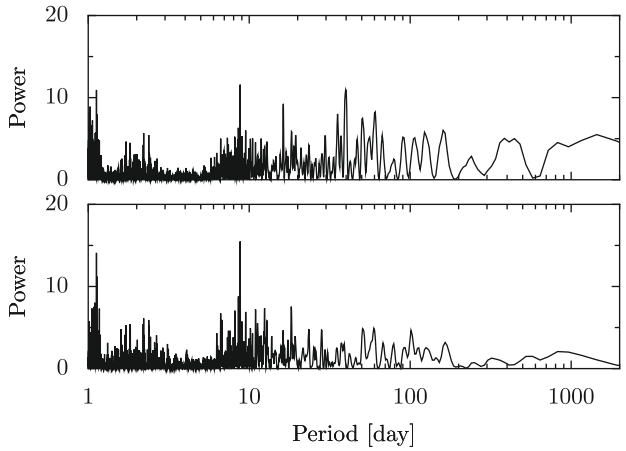

Fig. 2. Lomb-Scargle periodogram of the raw HARPS radial velocities (*top panel*), and of the velocities after subtraction of the 40-day signal (*bottom panel*).

Table 3. Orbital elements for the two-Keplerian orbital model of Gl 176.

Element	Value	Standard error
γ	26.4105 km s^{-1}	0.0004
P_1 [days]	8.7836	0.0054
e_1	0.0	Fixed
om$_1$ [deg]	0.0	Fixed
$T0_1$ [jdb]	2 454 399.79	0.33
$K1_1$ [m s^{-1}]	4.12	0.52
P_2 [days]	40.00	0.11
e$_2$	0.0	Fixed
om$_2$ [deg]	0.0	Fixed
$T0_2$ [jdb]	2 454 291.07	1.31
$K1_2$ [m s^{-1}]	4.23	0.53

3. Orbital analysis

Our radial velocity measurements do show coherent structure, and a Lomb-Scargle periodogram (Press et al. 1992) shows two narrow peaks around 8.8 and 40 days (Fig. 2, top panel). The two peaks have similar false-alarm probabilities of 0.1%, and their spacing is well removed from any significant feature in the window function. We therefore analyzed them simultaneously and searched for 2-planet Keplerian solutions with *Stakanof* (Tamuz, in prep.), a program which uses genetic algorithms to efficiently explore the large parameter space of multi-planet models. *Stakanof* robustly converged to a 2-Keplerian solution with periods that match the two periodogram peaks. Subtracting the longer period signal from the velocities increases the significance of the 8.8-day period in the periodogram (Fig. 2, lower panel), further increasing our confidence that this signal is real. Subtracting the short-period signal, on the other hand, produces a periodogram (not shown) with a less convincing 40-day peak.

The 2-planet model describes our measurements well, but certainly not perfectly (σ = 2.5 m s^{-1}, $\sqrt{\tilde{\chi}^2}$ = 2.46 per degree of freedom). A Lomb-Scargle periodogram of the residuals of this 2-planet solution, however, shows no significant peak. The significant residuals therefore contain no immediate evidence for an additional component.

Both Keplerian signals have amplitudes of ~4 m s^{-1}, which with hindsight is well under the sensitivity limit of Endl et al. (2008). Neither of their eccentricities is significant, and we therefore adopt circular orbits as our preferred solution (Table 3, Fig. 3). That choice does not affect any of our conclusions. The inner and outer planets, in a Keplerian interpretation of the radial velocity variations, have minimum masses ($m \sin i$) of 8 and 14 $M_{\rm Earth}$, and projected semi-major axes of 0.066 and 0.18 AU.

4. Activity analysis

Apparent Doppler shifts unfortunately do not always originate in the gravitational pull of a companion, because stellar surface inhomogeneities, such as plages and spots, can break the balance between light emitted in the red-shifted and the blue-shifted parts of a rotating star. These inhomogeneities then translate into rotationally modulated changes of both the shape and the centroid of spectral lines (e.g. Saar & Donahue 1997; Queloz et al. 2001). The activity level of Gl 176 is similar to that of Gl 674 (Fig. 4), where a spot is responsible for a 5 m s^{-1} radial velocity signal (Bonfils et al. 2007).

For well-resolved rotational broadenings, correlated variations in the shape, parametrized by the span of the line bisector, and in the centroid provide an excellent diagnostic of such apparent velocity variations. We do, however, measure a rotational velocity of $v \sin i \lesssim 0.8$ km s^{-1} from our Gl 176 spectra. This low rotation velocity removes much of the usual power of the bisector test, since the bissector span scales with a much higher power of $v \sin i$ than the centroid (Saar & Donahue 1997; Bonfils et al. 2007).

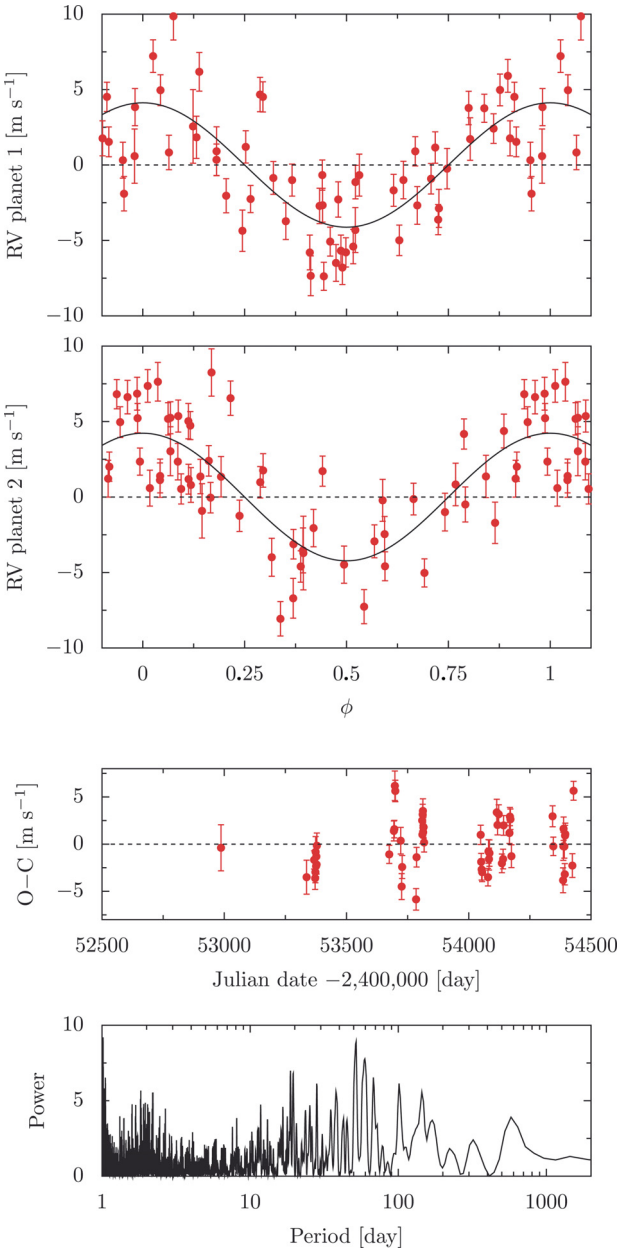

Fig. 3. *Top two panels:* radial velocity measurements phased to each of the two periods, after subtraction of the other component of our best 2-planet model. *Third panel:* residuals of the best 2-planet fit as a function of time (O−C, Observed minus Computed). *Bottom panel:* Lomb-Scargle periodogram of these residuals.

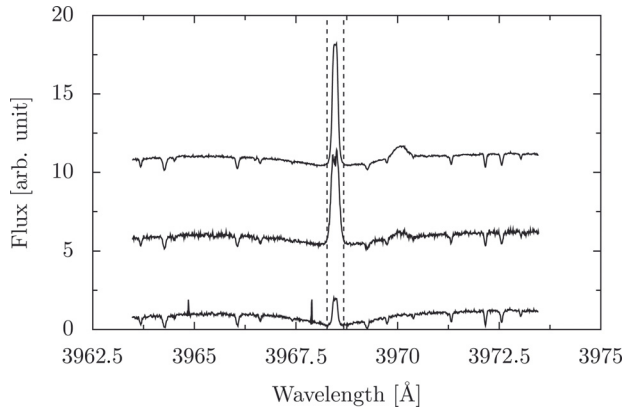

Fig. 4. Emission reversal in the Ca II H line in the average spectra of Gl 674 (M2V, *top*), Gl 176 (M2.5V, *middle*), and Gl 581 (M3V, *bottom*). Within our 100 M dwarfs sample, Gl 581 has one of the weakest Ca II emission and illustrates a very quiet M dwarf. Gl 674 and Gl 176 have much stronger emission and are both moderately active.

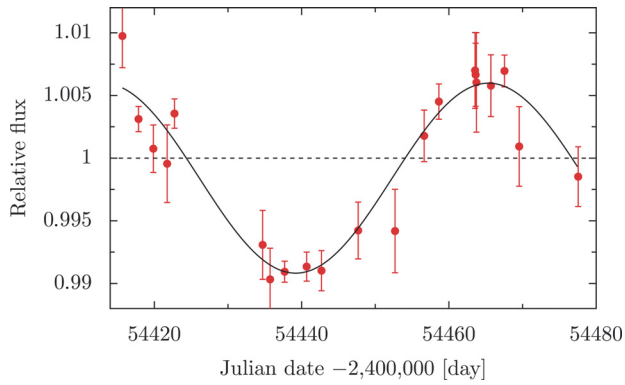

Fig. 5. *Upper panel*: differential photometry of Gl 176 as a function of time. The star clearly varies on a 40–50 days time scale with a ∼1.3% peak to peak amplitude.

Spots fortunately also produce flux variations, and they typically affect spectral indices, whether designed to probe the chromosphere (to which photospheric spots have strong magnetic connections) or the photosphere (because spots have cooler spectra). We therefore investigated the magnetic activity of Gl 176 through photometric observations (Sect. 4.1) and through a detailed examination of the chromospheric features in the clean HARPS spectra (Sect. 4.2).

4.1. Photometric variability

We obtained photometric measurements with the EulerCAM CCD camera of the Euler Telescope (La Silla) during 21 nights between November 10, 2007 and January 11, 2008. Gl 176 was observed through an I_c filter, to maximize the flux of both Gl 176 and an M star in the 11.7′ field of view, which we planned to use as photometric reference. That planned reference, however, proved variable, and we had to fall back to the average of two fainter blue stars, with a summed flux of only 7% of that of Gl 176. In retrospect, this filter choice was suboptimal. To minimize atmospheric scintillation noise, we took advantage of the low stellar density to defocus the images to *FWHM* ∼ 8″, so that we could use longer exposure times. The increased read-out and sky background noises from the larger synthetic aperture that we had to use remain negligible compared to both stellar photon noise and scintillation.

We gathered 5 to 7 images per night with a median exposure time of 31 s, except on December 29 when we obtained sets of 5 images at three well-spaced airmasses to measure the differential extinction coefficient. We tuned the parameters of the IRAF DAOPHOT package (Stetson 1987) and optimized the set of reference stars to minimize the average dispersion in the Gl 176 photometry during the individual nights. These parameters were then fixed for the analysis of the full data set. The nightly lightcurves for Gl 176 were normalized by those of the sum of the two references, clipped at 3-σ to remove a small number of outliers, and averaged to one measurement per night to examine the long-term photometric variability of Gl 176. Gl 176 clearly varies with a ∼1.3% peak-to-peak amplitude, and a 40–50 day (quasi-)period (Fig. 5). To verify that this variability

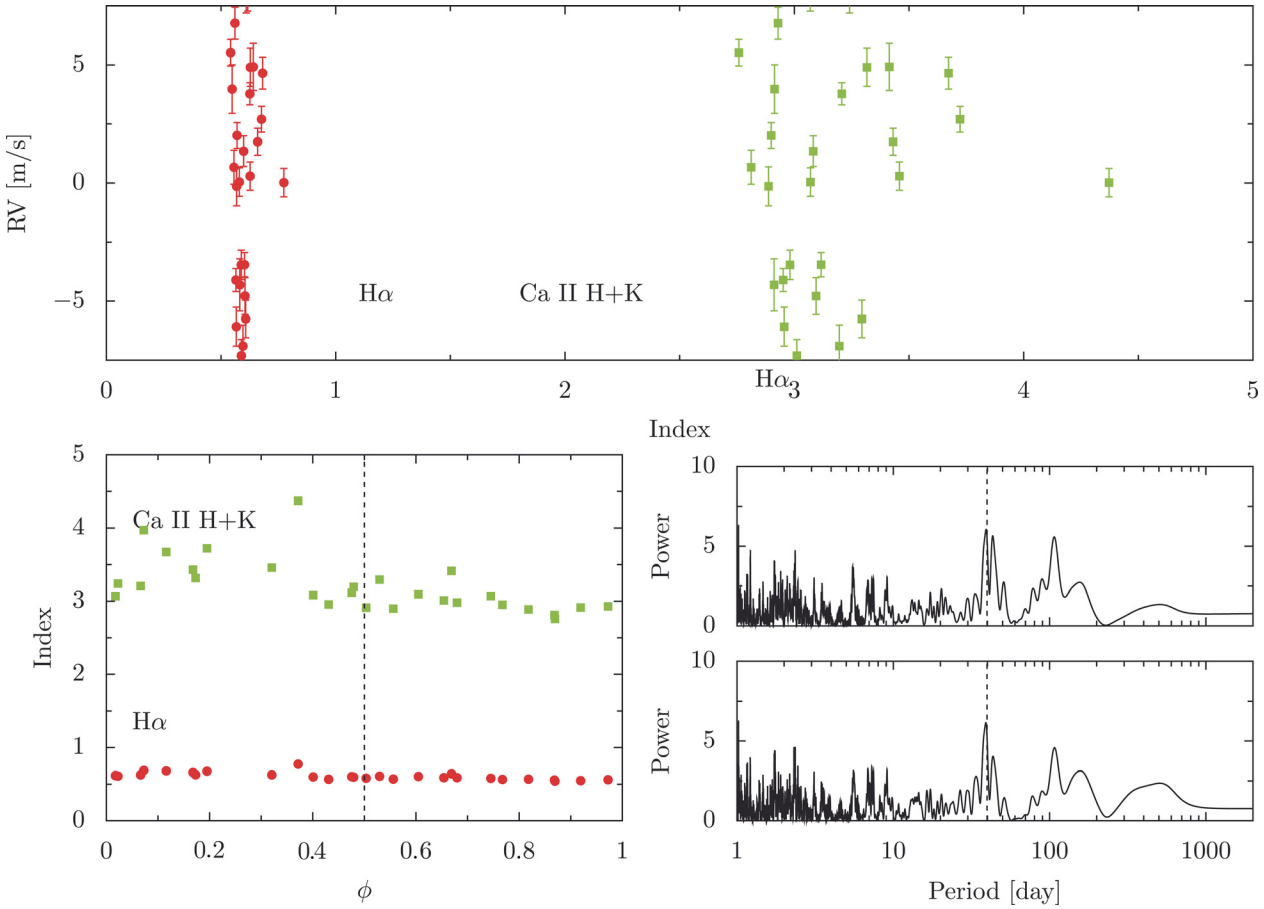

Fig. 6. *Upper panel*: differential radial velocity of Gl 176, corrected for the signature of the 8.8 days planet in our 2-planet fit, as a function of the Hα (red filled circles) and Ca II H&K (green filled squares) spectral indices defined in the text for the 2007/2008 observing season. *Bottom right panels*: the Ca II H+K and Hα indexes phased to the longer period of the 2-planet model. *Bottom left panels*: power density spectra of the spectroscopic indices. A clear power excess peaks at 40 days (vertical dashed lines).

does not actually originate in one of the reference stars, we repeated the analysis using each of the two reference stars. Those alternate lightcurves are very similar to Fig. 5. The variations are fully consistent with the 38.92-day period identified by Kiraga & Stepien (2007) in a much longer photometric timeseries. Our photometry demonstrates that Gl 176, which Kiraga & Stepien (2007) find did not significantly vary until JD = 2 453 300, has remained strongly spotted until the end of our radial velocity measurements, and it establishes the phase of the variations at a recent epoch. Our dense sampling also excludes 38.92 days having been an alias of the true period. We adopt the better defined Kiraga & Stepien (2007) value as the rotation period of Gl 176.

Our photometric observations are consistent with the signal of a single spot, within the limitations of their incomplete phase coverage: the variations are approximately sinusoidal, and their ~0.2–0.3 phase shift from the corresponding radial velocity signal closely matches the difference expected for a spot. The spot would cover 2.6% of the stellar surface if completely dark, corresponding to a ~0.16 $R_\star$ radius for a circular spot.

4.2. Variability of the spectroscopic indices

The emission reversal in the core of the Ca II H&K resonant lines and in the Hα line results from non-radiative heating of the chromosphere, which is magnetically coupled to the photospheric spots and plages. To probe these chromospheric spectral features, we measured in the HARPS spectra the spectral indices defined by Bonfils et al. (2007), and here we examine their variability.

The power spectra for both the H+K and Hα indices have clear peaks near 40 days (Fig. 6, lower right panel). Within the combined uncertainties, these peaks are consistent with both the photometric period and the longer radial velocity period. The phasing of the chromospheric index and the photometry is such that lower photometric flux matches higher Ca II emission, as expected if active chromospheric regions hover above dark photospheric spots.

Though certainly not as clearly as for Gl 674 (Bonfils et al. 2007), a plot of the (apparent) radial velocity (after subtraction of the 8.8-day planet) against the H+K spectral index (Fig. 6, upper panel) similarly suggests the loop pattern expected for a spot (Bonfils et al. 2007). A spot produces maximal velocity offsets when it is on either edge of the star, where geometric projection reduces the apparent area of its associated chromospheric emission to an intermediate value. It produces no velocity offset when it crosses the sub-observer meridian, with a maximal projected area for a front-facing crossing and a minimal (null for a non-polar spot) projected area for a back-facing crossing. The radial velocity offset therefore cancels for both the minimum and the maximum chromospheric emission, and is maximal for

intermediate chromospheric emission levels. The pattern here is definitely noisier than observed on Gl 674, suggesting that the spot pattern may evolve on a time scale similar to our observing period.

4.3. Planets vs. activity

In Sect. 3 we showed that our 57 radial-velocity measurements of Gl 176 are described well by two Keplerian signals. Section 4 however demonstrates that the rotation period of Gl 176 coincides with the longer of these two Keplerian periods. The stellar flux and the Ca II H+K emission vary with that period, with a phase relative to the velocity variations consistent with a magnetic spot on the stellar surface. As a consequence, some, and probably all, of the 40-day radial-velocity signal must originate in the spot. Planet-induced activity through magnetic coupling (e.g. Shkolnik et al. 2005) would in principle be an alternative explanation for the correlation, but it has never been observed for such a long-period planet. The inner planet in addition is hardly less massive than the hypothetical 40-day planet. One would, at least naively, expect its position in the inner magnetosphere of Gl 176 to more than make up for its lower mass. The 8.8-day period, however, is only seen in the radial velocity signal, and it has no photometric or chromospheric counterpart.

5. Discussion and conclusions

The most important result of the above analysis is that an $M \sin(i) = 8.4\ M_{\rm Earth}$ planet orbits Gl 176 in a ~8.8-day orbit. Variability identifies the stellar rotation period as 38.92 days, and the 8.8-day period therefore cannot reflect rotation modulation. In spite of its similar amplitude, the short-period signal also has no counterpart in either photometry or chromospheric emission, further excluding a signal caused by magnetic activity.

Like Gl 674 (Bonfils et al. 2007), Gl 176 demonstrates that single planets can be identified around moderately active M-dwarfs, at the cost of doubling or tripling the number of measurements over a magnetically quiet M-dwarf. Since the Keplerian model does not reflect a physical reality for the 40-day period, its residuals must be interpreted with caution. They are well above the measurement errors ($\bar{\chi}^2 = 5.86$ per degree of freedom) and could in principle reflect additional planet(s) in the system. More likely, these residuals mostly stem from long-term evolution of the spot pattern of Gl 176. Many additional radial velocity measurements would be needed to firmly identify additional planets among this spot-evolution noise. That cost may, in practice if not in theory, effectively impede the detection of multi-planet systems around moderately active stars. It may therefore not be fully by coincidence that Gl 674 and Gl 176 are simultaneously the only M-dwarf planetary systems with no indications of additional planets and the two most active M-dwarfs with known planets.

At 0.066 AU from its parent star, the thermal equilibrium temperature of Gl 176 b is ~450 K. Its 8.4 $M_{\rm Earth} M \sin(i)$ might be sufficient for accretion of a significant gas envelope to have occurred, in particular in case the inclination turns out to be non-trivial, but the rocky core most likely dominates its total mass (e.g. Seager et al. 2007; Valencia et al. 2007).

With a mass of only $M \sin(i) = 8.4\ M_{\rm Earth}$, Gl 176b adds to the growing evidence (e.g. Bonfils et al. 2007) that super-Earths are common around very low-mass stars: 6 of the 20 known planets with $M \sin(i) < 0.1\ M_{\rm Jup}$ orbit an M dwarf, in contrast to just 3 of the ~250 known Jupiter-mass planets.

Acknowledgements. We would like to thank the ESO La Silla staff for their excellent support and our collaborators of the HARPS consortium for making this instrument such a success, as well as for contributing some of the observations. Financial support from the "Programme National de Planétologie" (PNP) of CNRS/INSU, France, is gratefully acknowledged. X.B. acknowledge support from the Fundao para a Cincia e a Tecnologia (Portugal) in the form of a fellowship (reference SFRH/BPD/21710/2005) and a program (reference PTDC/CTE-AST/72685/2006), as well as the Gulbenkian Foundation for funding through the "Programa de Estmulo Investigao". N.C.S. would like to thank the support from Fundação para a Ciência e a Tecnologia, Portugal, in the form of a grant (references POCI/CTE-AST/56453/2004 and PPCDT/CTE-AST/56453/2004), and through program Ciência 2007 (C2007-CAUP-FCT/136/2006).

References

Bonfils, X., Delfosse, X., Udry, S., Forveille, T., & Naef, D. 2006, in Tenth Anniversary of 51 Peg-b: status of and prospects for hot Jupiter studies, ed. L. Arnold, F. Bouchy, & C. Moutou, 111
Bonfils, X., Delfosse, X., Udry, S., et al. 2005, A&A, 442, 635
Bonfils, X., Mayor, M., Delfosse, X., et al. 2007, A&A, 474, 293
Bouchy, F., Pepe, F., & Queloz, D. 2001, A&A, 374, 733
Delfosse, X., Forveille, T., Ségransan, D., et al. 2000, A&A, 364, 217
Endl, M., Cochran, W. D., Wittenmyer, R. A., & Boss, A. P. 2008, ApJ, 673, 1165
Johnson, J. A., Butler, R. P., Marcy, G. W., et al. 2007, ApJ, 670, 833
Kiraga, M., & Stepien, K. 2007, ArXiv e-prints, 707
Lovis, C., & Pepe, F. 2007, A&A, 468, 1115
Lovis, C., Mayor, M., Bouchy, F., et al. 2005, A&A, 437, 1121
Mayor, M., Pepe, F., Queloz, D., et al. 2003, The Messenger, 114, 20
Perryman, M. A. C., & ESA, eds. 1997, ESA Special Publication, 1200, The HIPPARCOS and TYCHO catalogues, Astrometric and photometric star catalogues derived from the ESA HIPPARCOS Space Astrometry Mission
Press, W. H., Teukolsky, S. A., Vetterling, W. T., & Flannery, B. P. 1992, Numerical recipes in FORTRAN, The art of scientific computing, 2nd Ed. (Cambridge: University Press)
Queloz, D., Henry, G. W., Sivan, J. P., et al. 2001, A&A, 379, 279
Saar, S. H., & Donahue, R. A. 1997, ApJ, 485, 319
Santos, N. C., Bouchy, F., Mayor, M., et al. 2004, A&A, 426, L19
Seager, S., Kuchner, M., Hier-Majumder, C. A., & Militzer, B. 2007, ApJ, 669, 1279
Shkolnik, E., Walker, G. A. H., Bohlender, D. A., Gu, P.-G., & Kürster, M. 2005, ApJ, 622, 1075
Skrutskie, M. F., Cutri, R. M., Stiening, R., et al. 2006, AJ, 131, 1163
Stetson, P. B. 1987, PASP, 99, 191
Upgren, A. R. 1974, PASP, 86, 294
Valencia, D., Sasselov, D. D., & O'Connell, R. J. 2007, ApJ, 656, 545